

# 論文 Studies of Shearing Behavior on Reinforced Concrete Beams with An Opening at Beam-End Region

Amadeo BENAVENT CLIMENT\*1, Masamichi OHKUBO\*2 and Tadao MATSUOKA\*1

**ABSTRACT:** Seven reinforced concrete beams with different shaped openings and different shear reinforcement were tested to study the shear transferring behavior in the vicinity of the opening. The beams behaved with shear failure pattern after flexural yielding. The beams with a circular opening performed better than the beams with a diamond or square opening. Non-linear finite element analyses were carried out to discuss the formation process of diagonal compression struts.

**KEYWORDS:** Beam with opening, Shear transferring, Compression strut.

## 1. INTRODUCTION

Beams are often pierced for piping or wiring of building equipment in the design of reinforced concrete buildings. A lot of experimental work has been carried out to study the shearing behavior of beams with openings, and some equations to predict the ultimate shearing strength of the beams have been developed as well. One of the equations called Hirosawa Equation, is an empirical equation modified from the Arakawa Equation for beams without opening.[1] In the equation called Ichinose Equation, a truss mechanism consisting of compression struts, ties and longitudinal steels is assumed to transfer shear force.[2] In the equation called Tsumura Equation, a plastic theory is applied for steels and concrete and an upper bound theorem is adopted to obtain the maximum shear capacity.[3] These equations agree well with the past experimental data. In the past experimental work, however, almost all the specimens were beams with one opening which was located at mid span of the beam in where the stress condition was mainly dominated by shear force. In the equations above, the stress due to bending moment is not considered but only shear force.

The necessary issues to be studied about beams with openings are; 1)to test the beams under a bending/shearing combined stress condition, and 2)to investigate the shear transferring mechanism due to compression struts, stirrups and diagonal reinforcement.

Focussing on the issues mentioned above, a fundamental experimental work and a non-linear finite element analysis were carried out. This paper presents the results of the tests and analyses, and the shear transferring mechanism is discussed.

## 2. TEST SPECIMENS

---

\*1 Graduate student of Kyushu Institute of Design(KID)

\*2 Dept. of Environmental Design, KID, Dr., Member of JCI

The following seven test specimens were programed focussing mainly on the shape of opening and the arrangement of shear reinforcement; Model CO: with a circular opening and stirrups, Model CD: overlaid diagonal reinforcement on the Model CO, Model DO: with a diamond opening and stirrups, Model DD: overlaid diagonal reinforcement on the Model DO, Model SO: with a square opening and stirrups, Model SD: overlaid diagonal reinforcement on the Model SO, and Model SS: added horizontal reinforcement and small stirrups in the top and bottom remaining concrete of the Model SO.

The dimensions and the reinforcing of Model CO are shown in Fig.1. The specimen was a cantilever beam with a 20cm x 40cm cross section. The shear span ratio  $M/QD$  ( $M$ : bending moment,  $Q$ : shear force,  $D$ : overall depth of the beam) was 3.6. The ratio of the maximum vertical dimension of each opening to the overall depth of the beam,  $H_e/D$ , was about 0.31. The center of the opening was located at the mid depth of the beam section and distanced  $1D$  from the beam end. The shape of the opening and the arrangement of shear reinforcement for the Models CD, DD, SD and SS are shown in Fig.2. Table 1 shows the mechanical properties of concrete and reinforcing steels.

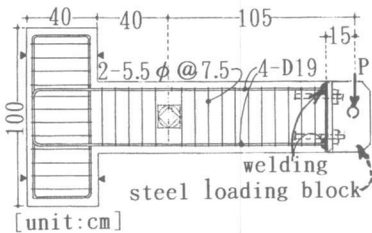


Fig.1: Specimens CO, DO, SO

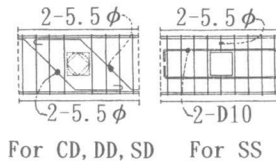


Fig. 2

Table-1: Material Property (kgf/cm<sup>2</sup>)

Concrete	$\sigma_B$	$\sigma_t$	$E_c (x10^5)$
	235	20.7	2.33
Steel	$\sigma_y$	$\sigma_t$	$E_s (x10^6)$
D19	3700	5513	1.72
D10	3660	5865	1.75
5.5φ	3000	5141	1.93

### 3. LOADING AND MEASURING TECHNIQUES

A monotonic load  $P$  was applied gradually at a distance 145cm from the beam end as shown in Fig.1. The corresponding increments of deflection at the loading point were +0.25mm and +3mm before and after the yielding of the longitudinal bars respectively. The strains of concrete and steels in the vicinity of opening were measured by strain gages as shown in Fig.3. The vertical, horizontal and diagonal deformation in the vicinity of the opening were also measured by displacement transducers.

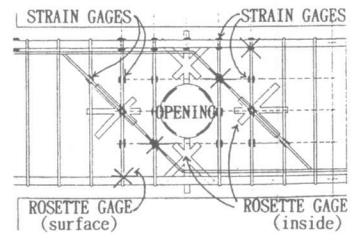


Fig. 3: Location of strain gages

### 4. LOAD DEFLECTION RELATIONSHIPS AND FAILURE BEHAVIOR

The relationships between the load  $P$  and the member deflection  $\delta$  at the loading point are shown in Fig.4. In the design, the test specimens were predicted to behave as a shear failure pattern in the vicinity of the opening without the flexural yielding of the longitudinal reinforcement according to the shear strength computed by Hirose and Ichinose equations, respectively. The failure patterns observed, however, were all flexural yielding before shear failure, because the concrete strength was higher than that in design. The specimens, except for the Model DD, failed with shear failure pattern at the member deflection of 2.4 through 5.6 times the deflection at flexural yielding, as shown in Table 2. The Model DD behaved as a flexural yielding pattern during the loading.

The final crack patterns of the Models CO, DO and SO are shown in Figs. 5a through 5c. The crack patterns of the Models CD, DD, SD and SS were similar to those of the models CO, DO and SO with the corresponding opening shape. The first shearing crack occurred at the lower left region of the opening, and the crack developed diagonally toward the bottom longitudinal reinforcement. The second shearing crack occurred at the upper right region of opening, and the crack developed diagonally toward the top longitudinal reinforcement. The final failure was dominated by the appearance of the third shearing crack in the upper remaining concrete region, and this triggered off the remarkable load reduction.

The difference in the opening shapes affected the deformation performance after flexural yielding as observed in Fig. 4 and Table 2. The beams with circular opening generally behaved better than the beams with diamond or square opening. The addition of diagonal reinforcement improved the deformation performance of the beams for each model.

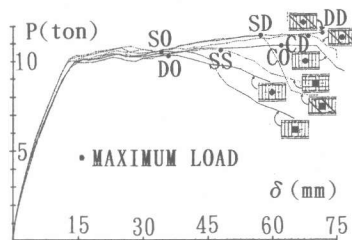


Table-2 Deflections at flexural yielding and maximum load, and ductility ratios

Specimens	CO	CD	DO	DD	SO	SD	SS
$\delta_y$ (mm)	15.0	12.8	14.8	12.9	13.9	13.4	13.9
$\delta_u$ (mm)	62.1	68.5	35.7	71.7	33.7	57.5	47.8
$\delta_u/\delta_y$	4.1	5.4	2.4	5.6	2.4	4.3	3.4

$\delta_y$ : Member deflection at flexural yielding  
 $\delta_u$ : Member deflection at maximum strength

Fig. 4: load deflection relationships

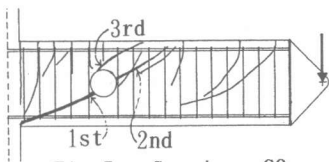


Fig. 5a: Specimen CO

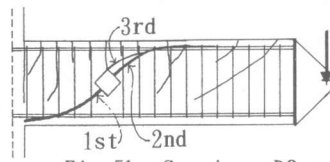


Fig. 5b: Specimen DO

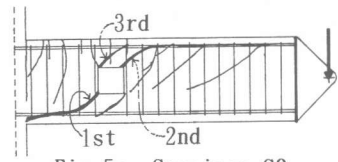


Fig. 5c: Specimen SO

## 5. ANALYSIS USING FINITE ELEMENT PROGRAM

The non-linear finite element analyses (FEM) were carried out to discuss the formation of compressive struts for shear transferring and the shearing contribution of stirrups or diagonal reinforcement in the vicinity of the opening. The computer program used was MARK5.2. The basic analytical model, meshing, and boundary conditions are shown in Fig. 6. Triangular elements with 6 nodes in the vicinity of opening and quadrilateral elements with 4 nodes for the other part of the specimen were used for concrete. Truss elements were used for steels. Plane stress condition was assumed. The "Smearred model" was adopted to represent concrete cracking. [4] To represent the shear transfer after cracking, a reduced shear modulus was used. The steel was modeled as a discrete element, and the effect of bond between concrete and steel was expressed by non-linear bond springs as shown in Fig. 7. [5]

The load deflection relationships analyzed for each specimen are shown in Fig. 8 comparing the responses tested. The loads for the first shearing crack, first yielding of shear reinforcement, flexural yielding and the stiffness at flexural yielding are listed with their corresponding test results in Table 3. Table 3 shows also the maximum load obtained by FEM assuming that the yielding stress of the longitudinal reinforcement is

infinite so flexural yielding is prevented. The maximum load computed in this way represents the ultimate shear strength, and is compared with that computed by Hirosawa and Ichinose equations in Table 3.

Although the behavior far beyond the flexural yielding was not analyzed because of the impossible convergence on computation, the load deflection curves analyzed up to the flexural yielding agreed well with the test results. The maximum load computed assuming that the yield stress of the longitudinal reinforcement is infinite, approximately agreed with the shear strength computed by Ichinose equation. The strengths computed by Hirosawa equation were generally conservative compared to measured results.

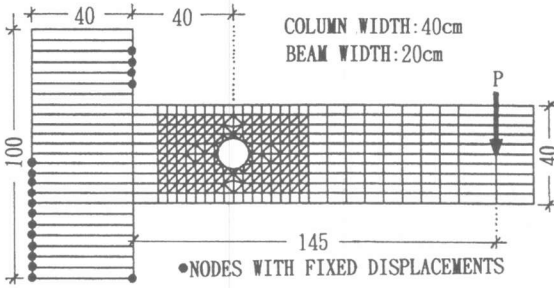


Fig. 6: Basic Analytical Model

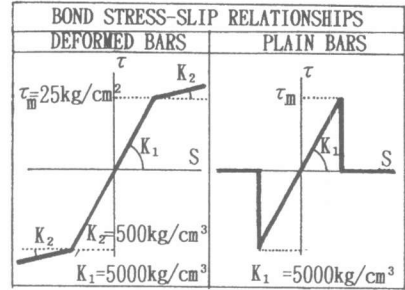


Fig. 7: Bond springs

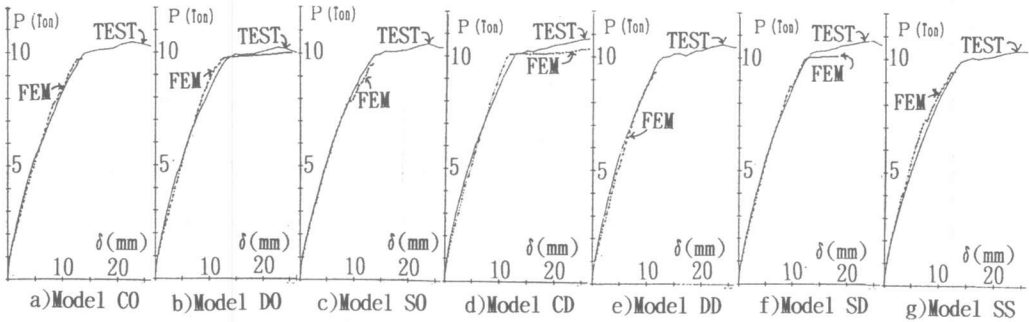


Fig. 8: Load deflection relationships analyzed and comparison with tests

Table-3 Comparison between tests and analyses

		Specimen	CO	CD	DO	DD	SO	SD	SS
$K_e$ : Elastic stiffness	$K_e$ Tests		21.3	23.6	20.4	24.0	20.3	23.0	25.8
	(t/cm) Analy.		27.3	27.4	27.1	27.2	26.9	27.2	27.1
$K_y$ : Stiffness at flexural yield	$K_y$ Tests		7.1	7.9	7.1	8.1	6.7	7.6	7.1
	(t/cm) Analy.		7.8	8.8	7.5	8.1	7.1	8.3	7.9
$P_{sc}$ : Load at first shear crack	$P_{sc}$ Tests		2.8	3.8	4.6	6.0	2.0	1.5	3.3
	(ton) Analy.		1.7	2.8	3.6	2.9	1.1	1.0	1.2
$P_{sy}$ : Load at first yield of shear reinforcement	$P_{sy}$ Tests		7.3	8.0	7.7	8.7	8.6	8.4	7.9
	(ton) Analy.		6.7	7.6	6.8	7.1	5.5	7.1	5.9
$P_y$ : Load at flexural yield	$P_y$ Tests		10.0	10.1	9.9	10.0	9.9	10.2	9.9
	(ton) Analy.		9.7	10.1	9.8	---	---	9.9	---
$P_{max}$ : Maximum load	$P_{max}$ Tests		10.9	11.5	10.3	11.6	10.6	11.4	10.7
	(ton) Analy.		10.2	11.3	---	---	---	---	---
Shear strength predicted by Hirosawa Eq. (ton)			7.7	9.2	---	---	---	---	---
Shear strength predicted by Ichinose Eq. (ton)			10.3	12.3	---	---	---	---	---

## 6. SHEAR TRANSFERRING DUE TO DIAGONAL COMPRESSION STRUTS

In this paragraph, the distribution of principal stress of the Model CO is focussed on to discuss the formation of compression struts in concrete. Figs.9a through 9d show the distribution of principal stress (compression). The dark shades in the figure identify the level of the compressive principal stress, and the darker the higher compressive stress. The small arrow represents the direction of the principal stress.

Fig.9a represents a state immediately after the first shearing crack. No obvious compression strut has been observed at this level, though a small diagonal compression belt is observed in the upper right region of the opening. Fig.9b represents the state after the second shearing crack appeared in the upper right region and developed diagonally. At this level, two diagonal belts, to be recognized as the "compression struts" are observed. The top end of the left compression strut focuses on the corner of the vertical stirrup and the top longitudinal reinforcement. Fig.9c represents the state immediately after the yielding of stirrups on both side of the opening, and Fig.9d represents the state immediately before the flexural yielding. It is observed through Figs.9b, 9c and 9d that the width of the compression strut increases as the load increases. The top end of the upper strut, which is supported by the vertical stirrups, widens along the upper longitudinal reinforcement after yielding of the vertical stirrups, and also the overall slope of the strut tends to incline. The formation of the diagonal compression struts to transfer shear force is quite similar to that assumed in the Ichinose model to compute the shear strength of beams with openings.

## 7. SHEAR FORCE TRANSFERRED THROUGH TOP AND BOTTOM CONCRETE OF OPENING

The analyzed shear forces transferred through the top and bottom remaining concrete of opening are shown in Table 4. The shear forces transferred through the top remaining concrete, in where the tension stress dominates due to bending moment, are less than 50%, but they are increasing as the load increases except for the models DO and DD. According to the tests, the final failure occurred in the top remaining region of the opening.

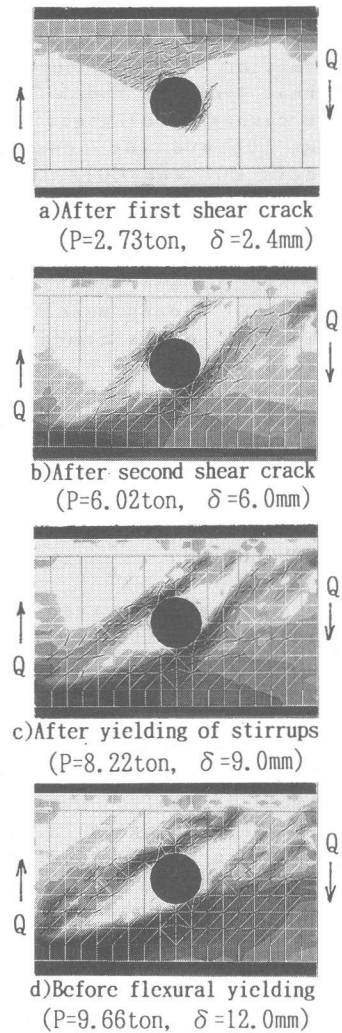


Fig.9: Principal Compressive Stress of Model CO

Table-4 Shear force shared by top and bottom concrete of opening (%)

Specimen	CO	CD	DO	DD	SO	SD	SS
Before shear crack ( $\delta=3\text{mm}$ )	Top	37	38	39	39	33	39
	Bot.	63	62	61	61	67	71
After shear crack ( $\delta=6\text{mm}$ )	Top	42	44	34	34	35	40
	Bot.	58	56	66	66	65	63
After stirrup yield ( $\delta=9\text{mm}$ )	Top	45	46	34	34	38	42
	Bot.	55	54	66	66	62	58

## 8. CONTRIBUTION OF SHEAR REINFORCEMENT FOR THE COMPRESSION STRUTS

Fig.10a shows the distribution of compressive principal stress for the Model CD with diagonal reinforcement. It represents the same deflection level as Fig.9d for the Model CO without diagonal reinforcement. The formation of the upper compression strut of the Model CD is a little different from the Model CO, and no obvious compression strut focussing toward the corner of diagonal reinforcement bent is observed.

Figs.10b and 10c represent the principal stress of two new analytical Models CO1 and CD1. The stirrup just beside the opening doubled in the Model CO1, and the diagonal reinforcement doubled in the Model CD1. In the Model CO1, two obvious compression struts which are focussing toward the top end of the stirrups appear separately in the upper left region. Comparing Figs10a and 10c it can be seen that the upper compression strut of the Model CD1 widens more than that of the Model CD due to the increase of the diagonal reinforcement. According to the analyses, the ultimate shear strength obtained by FEM assuming that the yielding stress of the longitudinal reinforcement is infinite, was a little larger for the Model CO1 than for the Model CD. This may indicate that the doubling stirrups just beside the opening is more effective than the adding the same amount of diagonal reinforcement.

## 9. CONCLUSIONS

1) The appearance of a diagonal crack in the remaining concrete region on the tension side due to bending moment, triggers off the ultimate failure in the beam with opening subjected to bending moment and shearing force.

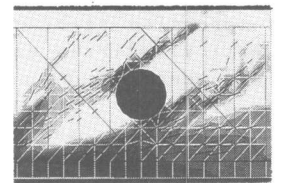
2) The beams with the circular opening showed better deformation performance than the beams with the diamond or square opening.

3) The diagonal compression struts are formed in both sides of the opening to transfer shear force from one side of the opening to the other. The end of the strut focuses toward the end of the stirrup beside the opening. The strut width increases and the slope of the strut inclines as the load applied increases.

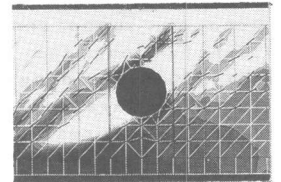
4) The doubling the stirrups beside the opening increases shear transferring more than adding the same amount of diagonal reinforcement.

## REFERENCES

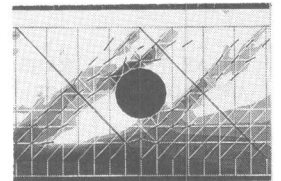
1. Hirosawa, M. and Shimizu, Y., "Seismic Performance of Reinforced Concrete Beams with Holes, Part 3", Summaries of Technical Papers of Annual Meeting of AIJ, 1978, pp. 1593-1594.
2. Ichinose, T. and Yokoo, S., "A shear design procedure of reinforced concrete beams with web openings," Summaries of Technical Papers of Annual Meeting of AIJ, 1990, pp. 319-322.
3. Tsumura, K., "Shear Behavior of Reinforced Concrete Beams with Openings", Trans. of AIJ, No. 407, 1990, pp. 47-60.
4. Rashid, Y. R., "Analysis of Prestressed Concrete Pressure Vessels," Nuclear Engineering and Design, Vol. 7, No. 4, April 1968, pp. 334-344.



a) Model CD  
( $P=10.1\text{ton}$ ,  $\delta=12.0\text{mm}$ )



b) Model CO1  
( $P=10.1\text{ton}$ ,  $\delta=11.7\text{mm}$ )



c) Model CD1  
( $P=10.2\text{ton}$ ,  $\delta=10.5\text{mm}$ )

Fig.10: Principal Compressive Stress